Thomas, D. D. (1985) in *The Enzymes of Biological Membranes* (Martonosi, A. N., Ed.) Vol. 1, pp 287–312, Plenum Publishing, New York.
Thomas, D. D. (1986) in *Techniques for the Analysis of Membrane Proteins* (Ragan, C. I., & Cherry, R. J., Eds.) pp 377–431, Chapman and Hall Publishers, London.
Thomas, D., Dalton, L. R., & Hyde, J. S. (1976) *J. Chem. Phys. 65*, 3006–3024.
Weast, R. C., Ed. (1961) *Handbook of Chemistry and Physics*, p 2227, The Chemical Rubber Co., Cleveland, OH.
Wenzel, H. R., Becker, G., & Goldammer, E. V. (1978) *Chem. Ber. 111*, 2453–2454.
Willingham, G. L., & Gaffney, B. J. (1983) *Biochemistry 22*, 892–898.
Wray, W., Boulikas, T., Wray, V. P., & Hancock, R. (1961) *Anal. Biochem. 118*, 197–203.

Sequence-Specific ^{1}H NMR Assignments and Secondary Structure of Porcine Motilin†

Nikhat Khan,‡ Astrid Graslund,‡,§ Anders Ehrenberg,‖ and John Shriver*,‡

Department of Medical Biochemistry, School of Medicine, and Department of Chemistry and Biochemistry, College of Science, Southern Illinois University, Carbondale, Illinois 62901, and Department of Biophysics, University of Stockholm, S-10691 Stockholm, Sweden

Received August 21, 1989; Revised Manuscript Received February 28, 1990

ABSTRACT: The solution structure of the 22-residue peptide hormone motilin has been studied by circular dichroism and two-dimensional ^{1}H nuclear magnetic resonance spectroscopy. Circular dichroism spectra indicate the presence of α-helical secondary structure in aqueous solution, and the secondary structure can be stabilized with hexafluoro-2-propanol. Sequence-specific assignments of the proton NMR spectrum of porcine motilin in 30% hexafluoro-2-propanol have been made by using two-dimensional NMR techniques. All backbone proton resonances (NH and αCH) and most of the side-chain resonances have been assigned by using double-quantum-filtered COSY, RELAYED-COSY, and NOESY experiments. Simulations of NOESY cross-peak intensities as a function of mixing time indicate that spin diffusion has a relatively small effect in peptides the size of motilin, thereby allowing the use of long mixing times to confidently make assignments and delineate secondary structure. Sequential αCH–NH and NH–NH NOESY connectivities were observed over a significant portion of the length of the peptide. A number of medium-range NOESY cross-peaks indicate that the peptide is folded into α-helix from Glu9 to Lys20, which agrees favorably with the 50% helical content determined from CD measurements. The intensities of selected NOESY cross-peaks relative to corresponding diagonal peaks were used to estimate a rotational correlation time of approximately 2.5 ns for the peptide, indicating that the peptide exists as a monomer in solution under the conditions used here.

Motilin is a small gastrointestinal peptide hormone (M_r = 2699) found in blood and in some endocrine cells situated in the gut (Usellini et al., 1984). The hormone stimulates gastrointestinal peristalsis, notably during the interdigestive period (Mutt, 1982; McIntosh & Brown, 1988; Schubert & Brown, 1974), and it has been associated with phase III of migrating myoelectric complexes (Jacobowitz et al., 1981). The receptors for the hormone are located primarily in the smooth muscle of the duodenum (Kondo et al., 1988). Elevated levels of the hormone are observed in many disorders, particularly diarrhea (Ohe et al., 1980; Imura et al., 1980; Christofides & Bloom, 1981).

Although numerous physiological and clinical studies have been performed on motilin, no crystallographic or solution structural data are available for this peptide hormone. Motilin is known to consist of a single peptide chain of 22 amino acids with the sequence FVPIFTYGELQRMQEKERNKGQ (Brown et al., 1973; Schubert & Brown, 1974). Recently it has been shown from corresponding cDNA sequences that human and porcine motilin have identical sequences (Dea et al., 1989). These studies also suggest that motilin is synthesized as a higher molecular weight precursor from which the 22 amino acid peptide is subsequently cleaved. The eight amino terminal residues are largely hydrophobic, while the remainder of the molecule can be classified as hydrophilic. Physiological studies on canine motilin reveal that the active portion of the molecule lies between residues 6 and 16 (Poitras et al., 1987). However, studies conducted with synthetic porcine motilin indicate that the whole molecule is responsible for biological activity (Ueda et al., 1977).

Two-dimensional nuclear magnetic resonance techniques have proven to be useful in the study of structural properties of small proteins and peptides (Wagner, 1983; Wuthrich, 1986; Wright et al., 1988). Through-bond or through-space connectivities are established either via spin–spin scalar coupling or through dipole–dipole interactions. Spin–spin scalar connectivities are visualized as correlation peaks in two-dimen-

† This study was supported by the Swedish Natural Science Research Council, Magn. Bergwalls Foundation, and Southern Illinois University School of Medicine. J.S. is a recipient of an NIH Research Career Development Award (AR01788).
* Author to whom correspondence should be addressed.
‡ Southern Illinois University.
§ Present address: Department of Medical Biochemistry and Biophysics, University of Umeå, S-90187 Umeå, Sweden.
‖ University of Stockholm.

0006-2960/90/0429-5743$02.50/0

sional homonuclear correlated spectra (COSY)[1] (Aue et al., 1976; Bax & Freeman, 1981) or two-dimensional relayed coherence transfer (RELAYED-COSY) experiments (Eich et al., 1982; Bax & Drobny, 1985). Dipole–dipole connectivities with interproton distances less than 5 Å are realized as correlation peaks in two-dimensional nuclear Overhauser enhancement spectroscopy (NOESY) experiments (Jeener et al., 1979). Distance constraints determined from 2D NOESY spectra can form the basis for three-dimensional structure determinations using distance geometry methods (Havel & Wuthrich, 1985; Braun & Go, 1985) or restrained molecular dynamics calculations (Clore et al., 19877; de Vlieg et al., 1988).

In this paper we present the sequence-specific assignments of motilin in 30% hexafluoro-2-propanol. Fluorinated alcohols such as hexafluoro-2-propanol and trifluoroethanol have been used in solution studies of a number of peptides (Clore et al., 1986; Tappin et al., 1988; Gooley & MacKenzie, 1988; Bazzo et al., 1988). It has been argued that these compounds do not create new secondary structures but actually stabilize α-helices which exist normally in aqueous solution in rapid equilibrium with random coil (Nelson & Kallenbach, 1986; Dyson et al., 1988b). This is most likely true except in sequences that have nearly equal tendencies to exist as α-helix or β-sheet, in which case the equilibrium will be shifted in favor of helix. We have used HFP here to facilitate the assignment of the NMR resonances to specific residues. Results obtained in the absence of fluorinated alcohol will be presented elsewhere.

Materials and Methods

Porcine motilin was kindly provided by Professor Viktor Mutt of Karolinska Institute, Stockholm, Sweden. It was prepared essentially as described earlier (Brown et al., 1971, 1972), and its identity with the previous preparation was chekced by comparison of amino acid compositions. Hexafluoro-2-propanol-d_2 (98% D) was obtained from Cambridge Isotope Laboratories. D_2O (99.98% purity) and acetic acid-d_3 (99.5 atom % D) were obtained from Aldrich. NMR sample tubes (535-PP) of 5-mm outer diameter were obtained from Wilmad Glass Co.

Circular dichroism spectra were recorded on a Jasco J-600 spectropolarimeter using a cuvette with a 2-mm light path. The initial sample contained 28 μM motilin in 20 mM acetic acid, to which increasing amounts of HFP were added as indicated. The spectra were corrected for dilution. The spectra were also base line corrected.

Samples for 2D NMR studies were prepared by dissolving 5 mg of motilin in approximately 0.5 mL of H_2O. The pH was adjusted to 3.9 with a few microliters of 1 M CD_3COOD. The pH was determined with a Radiometer glass electrode and was not corrected for the deuterium isotope effect (Bundi et al., 1979). The final NMR sample volume was adjusted to 1 mL to give 1.8 mM motilin in 60% H_2O, 30% HFP, and 10% D_2O (v/v).

All NMR experiments were performed on a Varian VXR 500 spectrometer interfaced to a Varian VXR-4000 computer. Chemical shifts are referenced to the H_2O resonance at 4.80 ppm at 21 °C. The H_2O peak chemical shift was measured relative to sodium 4,4-dimethyl-4-silapentanesulfonate (DSS) in a separate experiment. Field-frequency lock was maintained by the 10% D_2O in the solvent.

Phase-sensitive double-quantum-filtered COSY spectra (Rance et al., 1983) and phase-sensitive NOESY spectra (States et al., 1982) were collected according to standard procedures. Phase-sensitive spectra were collected with the hypercomplex method (States et al., 1982). In all 2D COSY and NOESY experiments, 1024 data points were collected in the t_2 domain and zero-filled to 2048 points before Fourier transformation. In the t_1 domain, 360 time increments were collected and the data were also zero-filled to 2048 points. In general, 40 transients were averaged for each t_1 time increment. Spectral widths of 5000 Hz were collected in both dimensions. Mixing times of 90–450 ms were used in the NOESY experiments. Prior to Fourier transformation, the data were multiplied by a Gaussian apodization function with a small amount of additional resolution enhancement applied with a positive exponential. The intense water peak was removed in all experiments by saturation of the water resonance frequency during the relaxation delays, and in the NOESY experiments also during the mixing time (Wider et al., 1983). Both carrier and decoupler frequencies were set equal to the water resonance frequency in all experiments (Zuiderweg et al., 1986). A few double RELAYED-COSY spectra were used to confirm assignments and were collected by using standard procedures (Sauriol et al., 1987) with a total time for each relay step (i.e., $\tau/2-180°-\tau/2$) of 0.04 s. In the RELAYED-COSY experiments, 1024 data points were collected in the t_2 domain, and 512 increments were collected in the t_1 domain, with 64 transients averaged for each increment.

Simulations of the time dependence of the intensities of NOESY diagonal and cross-peaks have been calculated on a Macintosh II by using programs written in TrueBASIC with the Scientific Graphics library (Hanover, NH) and also in *Mathematica* (Wolfram Research). Copies of the programs are available from one of us (J.S.). The programs make use of the equations described by Keepers and James (1984), Massefski and Bolton (1985), and Boelens et al. (1989). Briefly, the programs provide the matrix of peak intensities, **A**, as a function of the NOESY mixing time, t_m:

$$\mathbf{A}(t_m) = \chi e^{-\lambda t_m} \chi^{-1} \tag{1}$$

where λ is a vector made up of the eigenvalues of the relaxation matrix, **R**, and χ is the matrix of eigenvectors of **R**. The elements of **R** are

$$R_{ii} = \sum_j \rho_{ij} + \rho^*$$

$$R_{ij} = \sigma_{ij} \tag{2}$$

ρ^* is the "leakage" rate to the lattice and is assigned the value 1 s^{-1} (Clore & Gronenborn, 1989). The individual rate constants are given by

$$\rho_{ij} = \frac{h^2\gamma_i^2\gamma_j^2}{(2\pi)^2 r_{ij}^6}[6J_2(\omega) + 3J_1(\omega) + J_0(\omega)]$$

$$\sigma_{ij} = \frac{h^2\gamma_i^2\gamma_j^2}{(2\pi)^2 r_{ij}^6}[6J_2(\omega) - J_0(\omega)] \tag{3}$$

where $J_0(\omega)$, $J_1(\omega)$, and $J_2(\omega)$ are the spectral densities that characterize the motion of the protein relative to the proton resonance frequency ω. Substitution of appropriate values for the distances r_{ij} and the rotational correlation time allows for a description of the buildup of the NOESY peaks as a function

[1] Abbreviations: NMR, nuclear magnetic resonance; NOE, nuclear Overhauser enhancement; NOESY, two-dimensional nuclear Overhauser enhancement spectroscopy; COSY, two-dimensional homonuclear correlation spectroscopy; DQF-COSY, double-quantum-filtered homonuclear correlation spectroscopy; HFP, hexafluoro-2-propanol; RELAYED-COSY, relayed coherence-transfer spectroscopy; CD, circular dichroism; ppm, parts per million.

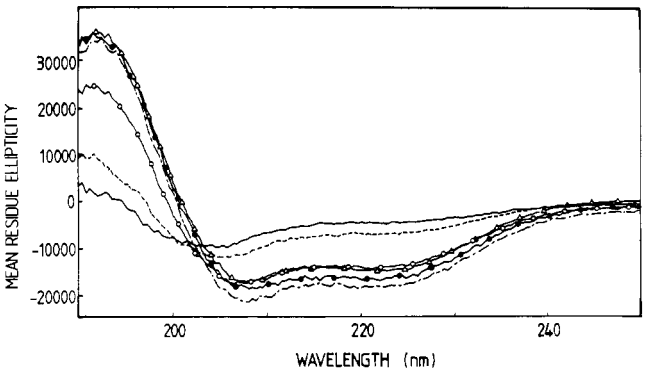

FIGURE 1: Circular dichroism spectra of porcine motilin collected in 20 mM acetic acid (pH 3.3) in the presence of various amounts of hexafluoro-2-propanol at 22 °C. The mean residue ellipticity is reported as deg·cm^2/dmol. The protein concentration was 27 μM. The hexafluoro-2-propanol concentration was 0% (—), 5% (---), 10% (○), 15% (△), 30% (- - -), and 40% (●).

of t_m. Conversely, if a given distance is known, the magnitude of a cross-peak relative to a corresponding diagonal peak (at a given mixing time) may be used to estimate the rotational correlation time.

Results

Circular Dichroism. Figure 1 shows a series of CD spectra of motilin collected in the presence of various concentrations of hexafluoro-2-propanol (HFP). There is a significant increase in both the positive and the negative CD bands with increasing HFP concentration. The intensity at 222 nm changes from a mean residue ellipticity of −4300 deg·cm^2/dmol at 0% HFP to −18 000 deg·cm^2/dmol at 30% HFP. No further increase in ellipticity is observed above 30% HFP. Other CD spectra indicate that the increased intensity induced by HFP can be abolished with the addition of 6 M guanidinium hydrochloride (data not shown).

Initial NMR Spin System Identification, Assignments, and Connectivities. Assignment of the NMR resonances of valine 2, isoleucine 4, threonine 6, and leucine 10 can be initiated by noting the methyl resonances in the high-field region (Figure 2). There is only one copy of each of these residues in porcine motilin, which further facilitates identification.

Isoleucine 4 is easily assigned due to its characteristic spin system (Wuthrich, 1986). All isoleucine 4 resonances can be unambiguously assigned at this stage except for the NH resonance for which there are two potential αCH–NH NOESY cross-peaks (amide proton at 7.09 or 8.17 ppm), and the high-field connectivities are outlined in Figure 2. Likewise, the spin system of valine 2 is easily found. The NOESY connectivity between the Val2 NH and the N-terminal Phe1 αCH is observed in the fingerprint region at 4.2, 7.53 ppm.[2]

This leaves a single high-field cross-peak which can be assigned to δCH_3–γCH_2 of leucine 10. The NH resonance of leucine 10 was not assigned at this point since the COSY spectrum showed three possibilities (7.92, 8.22, and 8.39 ppm) for its assignment (see below for the final assignment).

In the COSY spectrum at 21 °C only three cross-peaks were observed in the region expected for αCH–βCH_2 cross-peaks of aromatic amino acids [i.e., approximately 3.2, 4.2 ppm: a pair of cross-peaks and a single intense cross-peak (data not shown)]. Two pairs of αCH–βCH_2 cross-peaks near the H_2O signal were "bleached out" due to high-power irradiation of the water signal as described by Kumar et al. (1980). However, these peaks were clearly observed in 100% D_2O at 5 °C (data not shown) and also in DQF-COSY and NOESY experiments.

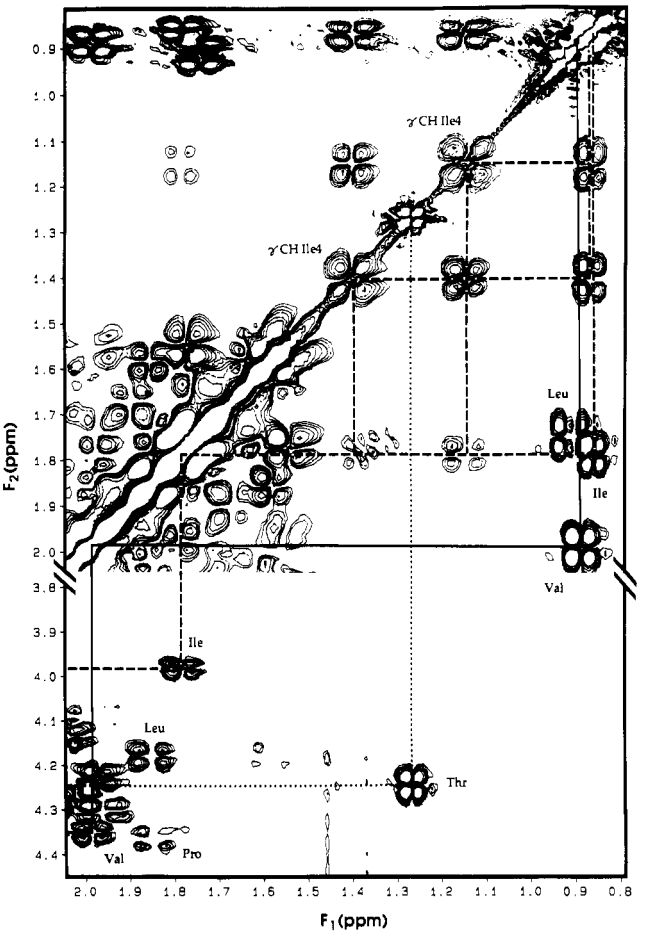

FIGURE 2: High-field region of the 500-MHz ^{1}H COSY spectrum of porcine motilin. The protein concentration was 1.8 mM in 30% HFP, 60% H_2O, and 10% D_2O at pH 3.9 and 21 °C. Selected J-connectivities are indicated for valine 2 (—), isoleucine 4 (- -) and threonine 6 (···).

Figure 3 illustrates the assignment procedure for the two phenylalanines, tyrosine, and asparagine using NOESY connectivities. These are the only examples of AMX spin systems in motilin. Note that the long mixing time used in this experiment gives some of the advantages of a RELAY experiment. The NOESY cross-peak at 4.13, 7.94 ppm in the fingerprint region (Figure 4) allows connection of the Tyr7 to Thr6. In a NOESY experiment with a long mixing time (450 ms), an obvious pair of cross-peaks with F_1 coordinates of 2.83 and 2.95 ppm is seen at the F_2 levels of 6.84, 7.61, and 7.99 ppm (Figure 3). This is a typical pattern for asparagine (Wuthrich, 1986). The two γNH_2 protons have different chemical shifts and are connected by a strong NOESY (and also a COSY) cross-peak at 6.84, 7.61 ppm. The assignment of the amide proton is straightforward from the lower pair at 7.99 ppm. The assignment of the αCH is accomplished similarly. It lies very close to the water signal, but it can be clearly seen in 100% D_2O.

The remaining two pairs of AMX αCH–βCH_2 cross-peaks must belong to the two phenylalanines. Since Phe1 forms the N-terminal residue of the molecule, it was inferred that the αCH which deviates most from the random coil value (Wuthrich, 1986) must be phenylalanine 5.

The two αCH–βCH_2 cross-peaks of Pro3 (not shown) are identified by the absence of a corresponding αCH–NH connectivity (since proline does not have an NH proton) along

[2] Cross-peak coordinates are referenced throughout as F_1 chemical shift vs F_2 chemical shift in ppm, i.e., F_1, F_2.

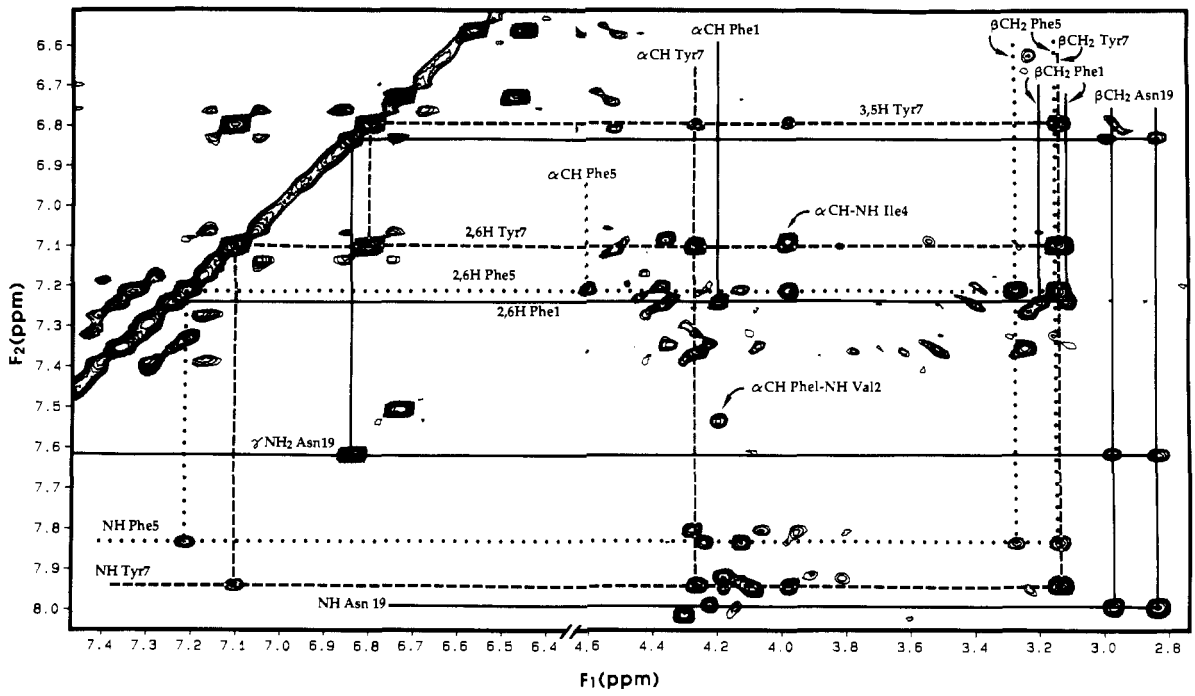

FIGURE 3: A portion of the 500-MHz ^{1}H NOESY spectrum of motilin showing the assignments and connectivities of the AMX spin systems. Sample conditions were as described in the legend of Figure 2, and the NOESY mixng time was 450 ms. The logic of the assignment of the aromatic residues of motilin is illustrated. The following selected connectivities are indicated: 2,6H, 3,5H, NH, αCH, and βCH$_2$ protons of tyrosine 7 (---); the NH, γNH, and βCH$_2$ protons of asparagine 19 (—); the 2,6H, αCH, and βCH$_2$ of phenylalanine 5 (···); and the 2,6H, αCH, and βCH$_2$ of phenylalanine 1 (—).

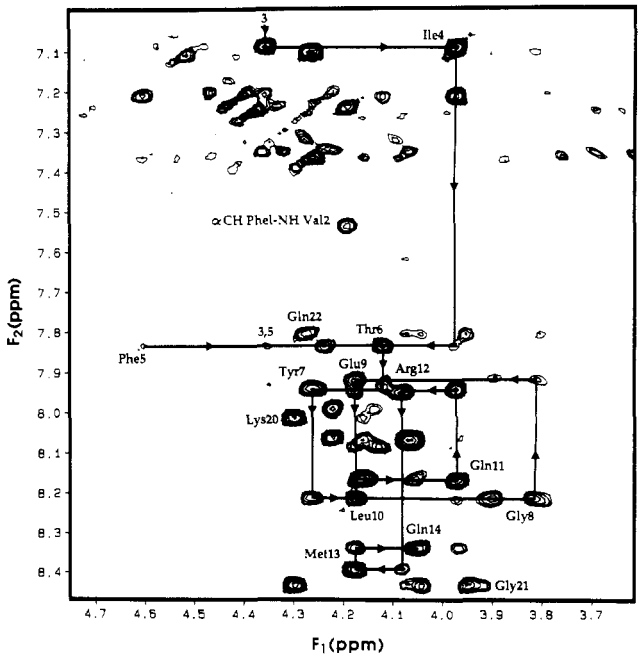

FIGURE 4: The αCH–NH cross-peak region of the 500-MHz ^{1}H NOESY spectrum of motilin. Sample conditions were as described in the legend of Figure 2 with a mixing time of 450 ms. Sequence-specific assignments from proline 3 to glutamine 14 via alternating αCH_i–NH_{i+1} and αCH_i–NH_{i+1} connectivities are shown with solid arrows.

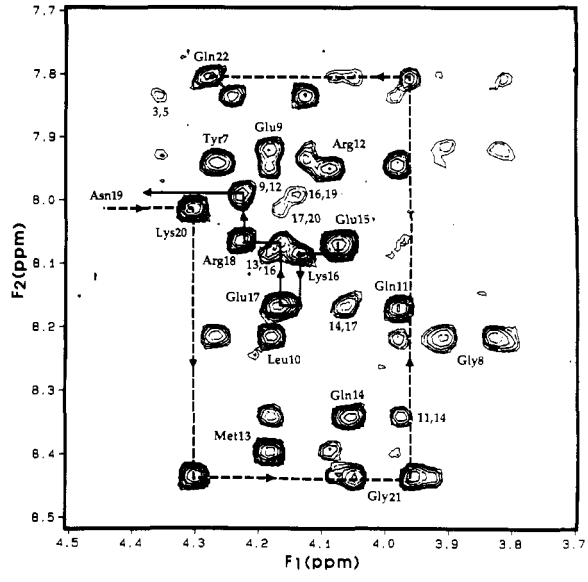

FIGURE 5: An enlarged section of the fingerprint region of the 500-MHz ^{1}H NOESY spectrum of motilin. Sample conditions were as in Figure 2. Backbone connectivities are shown from glutamine 15 to asparagine 19 and from lysine 20 to glutamine 22.

a 4.635 F_1 trace in the fingerprint region of the COSY spectrum in H_2O. The αCH–βCH$_2$ cross-peaks occur at 4.365, 1.85 ppm and 4.365, 2.22 ppm. Proline γCH$_2$–δCH$_2$ cross-speaks are prominently placed at 2.016, 3.55 ppm and 2.016, 3.72 ppm, as expected from chemical shift data for small peptides. The δCH$_2$ protons of proline 3 exhibit NOESY connectivities to Val2 γCH$_3$ and αCH at 0.87, 3.55 ppm, 0.87, 3.72 ppm and 3.55, 4.35 ppm, 3.72, 4.35 ppm, respectively. The NOESY connectivity between the αCH of valine 2 and the δCH$_2$ of proline 3 indicates that proline exists in a trans configuration (Dyson et al., 1988a). A strong NOESY cross-peak between Pro3 αCH and an NH is observed at 4.365, 7.09 ppm, thus allowing assignment of the Ile 4 NH.

The glycine 8 αCH$_2$ pair was assigned sequentially from tyrosine 7 via the NOESY cross-peak at 4.265, 8.215 ppm (Figure 4); i.e., the αCH of Tyr7 shows a NOESY connectivity to a NH resonance at 8.215 ppm, which in turn has connectivities to the two αCH protons of glycine 8 at 3.81 and 3.91 ppm. The other pair of cross-peaks at 3.94, 8.43 ppm and 4.05, 8.43 ppm, were assigned to glycine 21. In fact, there are two sets of Gly 21 NOESY cross-peaks in the fingerprint region (Figure 5): a major inner pair (at 3.96, 8.43 ppm, and 4.05, 8.43 ppm) with a minor pair (at 3.93, 8.43 ppm and 4.08, 8.43

Table I: Proton NMR Resonance Assignments of Porcine Motilin

residue	chemical shifts (ppm)[a] NH	αCH	βCH	others
Phe1		4.2	3.19, 3.11	2,6H, 7.245; 3,5H, 7.36; 4H, 7.35[b]
Val2	7.53	4.35	1.99	γCH_3, 0.87
Pro3		4.365	1.85, 2.22	γCH_2, 2.016, 2.016; δCH_2, 3.72, 3.55
Ile4	7.09	3.985	1.79	γCH_2, 1.39, 1.15; γCH_3, 0.854; δCH_3, 0.835
Phe5	7.84	4.61	3.28, 3.14	2,6H, 7.21; 3,5H, 7.34; 4H, 7.37
Thr6	7.84	4.13	4.24	γCH_3, 1.265
Tyr7	7.94	4.265	3.145	2,6H, 7.12; 3,5H, 6.8
Gly8	8.215	3.81, 3.91		
Glu9	7.92	4.18	2.15, 2.23	γCH_2, 2.4
Leu10	8.22	4.18	1.58, 1.85	γCH, 1.74; δCH_3, 0.88, 0.89
Gln11	8.17	3.98	2.12	γCH_2, 2.23, 2.28; δNH_2, 6.46, 6.565
Arg12	7.95	4.09	1.97, 2.06	δCH_2, 3.245; γCH_2, 1.66, 1.89; NH, 7.27; NH_2, 6.635
Met13	8.39	4.18	2.34, 2.24	γCH_2, 2.61, 2.74; ϵCH_3, 2.06
Gln14	8.34	4.05	2.235, 2.18	γCH_2, 2.6, 2.355; δNH_2, 6.47, 6.73
Glu15	8.07	4.07	2.19,[b] 2.225	γCH_2, 2.43, 2.495
Lys16	8.085	4.135	2.045	ϵCH_2, 3.03; δCH_2, 1.745; γCH_2, 1.61, 1.53
Glu17	8.16	4.165	2.19, 2.09	γCH_2, 2.46
Arg18	8.06	4.22	1.97	δCH_2, 3.255; γCH_2, 1.84, 1.74; NH, 7.36; NH_2, 6.67
Asn19	7.99	4.76	2.95, 2.83	γNH_2, 7.61, 6.84
Lys20	8.01	4.3	1.96	γCH_2, 1.55; δCH_2, 1.76; ϵCH_2, 3.08
Gly21	8.43	3.94, 4.05		
Gln22	7.8	4.275	2.235, 2.02	γCH_2, 2.37; δNH_2, 6.63,[b] 7.79[b]

[a] Chemical shifts are referenced relative to DSS. [b] Ambiguous assignment.

ppm). NOESY connectivities from glycine 21 lead straightforwardly to the assignment of the backbone protons of glutamine 22 and lysine 20 (Figure 5).

Glutamate 9 is simply assigned sequentially via the two NOESY cross-peaks from glycine 8 (Figure 4). Thus the amide and αCH resonances of this residue are assigned.

As indicated above, there were initially three choices for the amide proton of leucine 10. We found that only one of these can be connected to glutamate 9. From the NH–βCH_2 and NH–δCH_3 intraresidue NOESY connectivities, it can be concluded that the amide resonance of leucine 10 must be at 8.22 ppm.

This leaves the eight residues from glutamine 11 to arginine 18 to be delineated. The assignment of the two arginines (i.e., 12 and 18) was initiated by using the connectivities between the side-chain ϵNH resonances and the δCH_2 protons clearly observed in the COSY spectrum. Complete assignment of one arginine could be made by using the DQF-COSY map, and NOESY connectivities at a mixing time of 450 ms were considered to delineate the intraresidue couplings between the side-chain and αCH/NH resonances for the other arginine. Cross-peaks between backbone NH and γ and β protons were also seen. A strong NOESY cross-peak (at 4.22, 7.99 ppm) from the previously assigned NH proton of asparagine 19 to an αCH allows assignment of the first arginine to Arg18. By elimination, the other arginine must be residue 12.

Final Assignments (Table I). It seemed initially that the highly unusual COSY connectivity at 3.985, 7.09 ppm (Figure 4) was a reasonable choice for the intraresidue αCH–NH connectivity of Gln11 since there appeared to be a strong NOESY connectivity to the previously assigned arginine 12 amide proton. However, strong NOESY connectivities between an amide resonance at 8.17 ppm and the βCH_2 and γCH_2 leucine 10 resonances made the cross-peak at 3.98, 8.17 ppm the more logical choice for the αCH–NH connectivity of Gln11. The cross-peak from Gln11 αCH to Arg12 NH is not aligned perfectly for some unexplained reason. The assignment of the Gln11 NH allows the NOESY connectivity to Leu10 αCH to be made at 4.18, 8.17 ppm. This cross-peak is clearly composed of at least one other peak, and as shown below, it is actually three overlapping cross-peaks. The unusual cross-peak at 3.985, 7.09 ppm was now assigned to isoleucine 4, which was confirmed in particular by a RELAYED-COSY experiment and the NOESY connectivity in the fingerprint region to phenylalanine 5 (Figure 4). Thus the Ile4 NH resonance is shifted rather dramatically upfield and is noticeably far away from all the other NH peaks. In the absence of hexafluoro-2-propanol the Ile4 αCH–NH cross-peak was at 4.05, 8.09 ppm (data not shown).

Making the sequential assignment from residue 14 to 15 is not straightforward. Following the backbone connectivities entirely within the NOESY fingerprint region, the Gln14 intraresidue NH_i–αCH_i cross-peak connects through a well-isolated αCH_i–NH_{i+1} sequential cross-peak (at 4.05, 8.16 ppm) to a NH_i–αCH_i intraresidue cross-peak at 4.165, 8.16 ppm (Figure 5). This latter intraresidue cross-peak on the other hand could be sequentially connected through a sequential cross-peak to the NH_i–αCH_i intraresidue cross-peak of arginine 18; and in the reverse direction through a sequential cross-peak to the lysine 16 intraresidue cross-peak at 4.135, 8.085 ppm. This implies that the isolated αCH_i–NH_{i+1} peak at 4.05, 8.16 ppm does not lead from Gln14 to Glu15. The more probable assignment for the intraresidue cross-peak at 4.165, 8.16 ppm must be glutamate 17, and not glutamate 15. The logical solution is to assign the intense αCH_i–NH_i intraresidue cross-peak at 4.07, 8.07 ppm to glutamate 15. This implies that the intraresidue αCH–NH(15,15) and the αCH–NH(14,15) sequential cross-peaks are nearly coincident. To confirm this assignment, three-dimensional stack plot data were examined. It was observed that this cross-peak was significantly (3-fold) larger than neighboring peaks. Similarly, the stack plot shows that the now assigned intraresidue cross-peak of glutamate 17 at 4.165, 8.16 ppm is much more intense than adjacent resonances. This is consistent with our previous assignment of a sequential NOESY connectivity between residues 10 and 11 at 4.18, 8.17 ppm.

The backbone connectivity from Glu15 to Glu17 is completed by assigning the cross-peak at 4.135, 8.085 ppm to an intraresidue NH–αCH connectivity. This implies that the intense cross-peak noted above at 4.07, 8.07 ppm and 4.165, 8.16 ppm contains interresidue NOESY cross-peaks, i.e., each actually is composed of three cross-peaks, which is consistent with their intensities relative to other peaks in 3D stack plots. The NH–$\beta CH_2/\gamma CH_2$ region (Figure 6) was examined thoroughly in the long mixing time NOESY and in the DQF-COSY experiments in order to assign the glutamine 11, glutamine 14, glutamate 15, and glutamate 17 side-chain resonances.

Figure 7 depicts the NH–NH through-space connectivities for motilin. It is observed that most sequential connectivities seen in the αCH–NH region are also observed in this region, thereby substantiating the sequential assignments. Sequential NH_i–NH_{i+1} connectivities can be followed from isoleucine 4 to phenylalanine 5, from threonine 6 to leucine 10, from

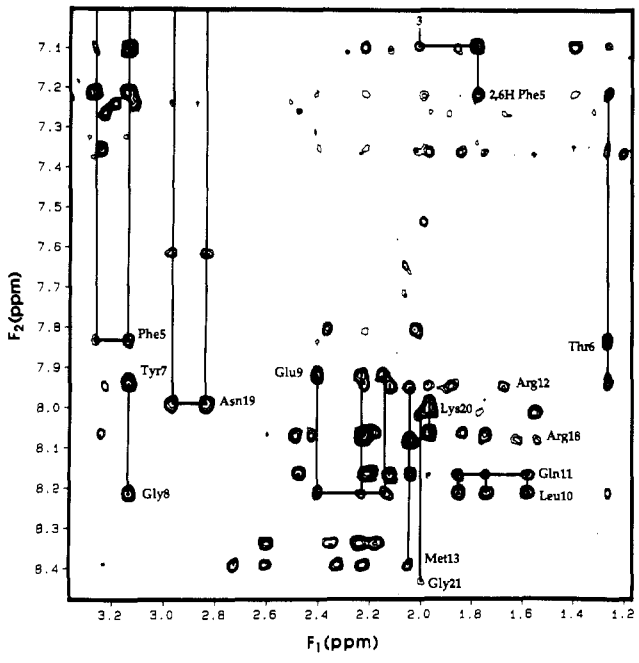

FIGURE 6: The βCH_2–NH and γCH_2–NH region of the 500-MHz ^1H NOESY spectrum of motilin. Sample conditions were as described in the legend of Figure 2. The vertical position of selected NH's on the 2D map are labeled. Connectivities between selected residues are indicated with solid vertical lines.

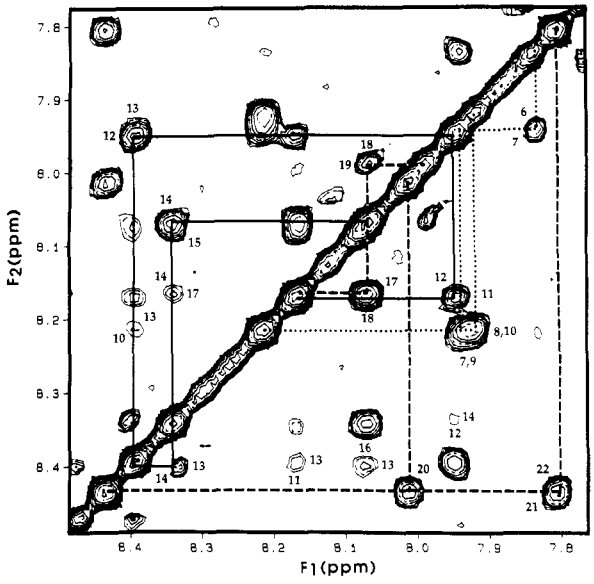

FIGURE 7: The NH–NH region of the NOESY spectrum of motilin. Connectivities NH_i–NH_{i+1} from residues 6 to 10, 11 to 15, 17 to 19, and 20 to 22 are outlined. The spectrum is symmetric about the diagonal, so for the sake of clarity, connectivities are indicated only on one side or the other. Some medium-range cross-peaks are also indicated. The mixing time for the experiment shown here was 450 ms.

glutamine 11 to glutamate 15, from glutamate 17 to asparagine 19, and from lysine 20 to glutamine 22. Sequential NH_i–NH_{i+1} cross-peaks due to 15, 16 and 19, 20 would be too close to the diagonal to observe, so their absence does not indicate that they do not exist. Likewise, 5 and 6 have the same chemical shift, and a cross-peak would not be observed. Noticeably absent is the 10, 11 NH–NH cross-peak.

Nonsequential NOEs. In addition to the sequential NOE cross-peaks observed, numerous connectivities were identified between distant residues on the peptide chain. Some of these are illustrated in Figures 5, 6, and 8. Of particular interest are those between residues i and $i + 3$. Such medium range

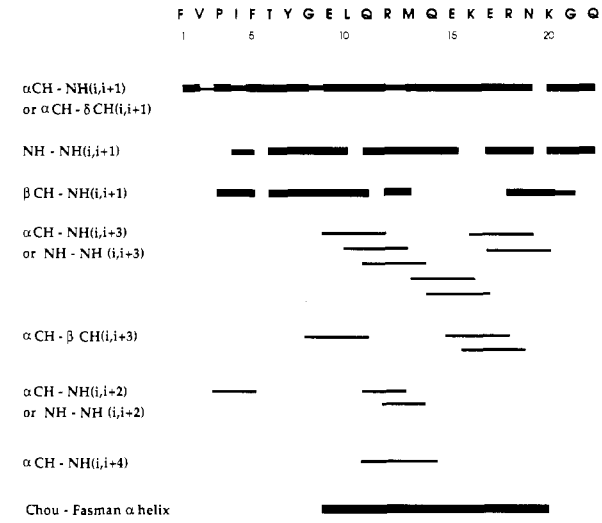

FIGURE 8: A graphical summary of the observed NOE connectivities in porcine motilin along with the region of the helix predicted by the Chou–Fasman procedure. The relative intensities of the cross-peaks are indicated by the bar width, except for the αCH–NH(i,i+1) connectivities where the narrowest bar indicates that the connectivities could not be observed due to overlap of resonances or the absence of an NH (in the case of proline 3).

i, $i + 3$ NOESY cross-peaks are observed in the fingerprint, amide–amide, and α–β regions of the NOESY spectrum. The ones in the fingerprint region are Glu9 αCH–Arg12 NH, Gln11 αCH–Gln14 NH, Met13 αCH–Lys16 NH, Gln14 αCH–Glu17 NH, Lys16 αCH–Asn19 NH, and Glu17 αCH–Lys20 NH. In addition, a few i, $i + 3$ cross-peaks were observed in the region F_1 = 1.0–3.0 ppm, F_2 = 3.0–4.8 ppm. These include Gly8 αCH–Gln11 βCH_2, Glu15 αCH–Arg18 βCH_2, and Lys16 αCH–Asn19 βCH_2. Medium-range NOESY cross-peaks were also observed in the amide–amide region: Leu10 NH–Met13 NH, Met13 NH–Lys16 NH, and Gln14 NH–Glu17 NH. A couple of weak NOESY cross-peaks between residues i, $i + 4$ and i, $i + 2$ were also observed in these regions. These are Ile4 αCH–Gly8 NH, Gln11 αCH–Glu15 NH, Pro3 αCH–Phe5 NH, Gln11 NH–Met13 NH, and Arg12 NH–Gln14 NH. Figure 8 presents a summary of the observed NOEs.

Two cross-peaks are seen in the NH–NH region of the NOESY spectrum which have not been assigned. These occur at 8.40, 8.48 ppm and 8.03, 8.11 ppm. There are no additional cross-peaks at these chemical shifts to peaks at higher field, indicating that these are not amino acid residues, and we attribute them to impurities in the sample.

Rotational Correlation Time and Spin Diffusion. We have measured the rotational correlation time of motilin in solution from the 2D NOESY data by using the integrated intensities of selected cross-peaks relative to a corresponding diagonal peak. The most convenient peaks for this purpose were the NOESY peaks which occur in uncrowded regions of the spectrum, allowing the measurement of both the diagonal and cross-peak intensities. The two δ protons of Pro3 are particularly good examples due to their proximity, viz., 1.78 Å, so that the NOESY peak intensities would be expected to be little affected by spin diffusion. The ratio of the diagonal peak intensity to the cross-peak intensity (collected at 90-ms mixing time) was compared to simulated data calculated by using either (1) a two-spin system with a separation of 1.78 or (2) an eight-spin system intended to model the vicinity of the δ protons of proline 3, i.e., the αCH and NH of valine 2 and the β, γ, and δ protons of proline 3 in an extended chain conformation. Similar results were obtained with either the

two-spin or eight-spin system, and the best fit of the data was obtained with a rotational correlation time of 1.2 ns.

The resonance of the amino proton of glutamine 14 is also isolated, and its cross-peak with its own αCH and the NH of glutamate 15 can be used in a similar manner. Two model spin systems were used: a 6-spin system and a 15-spin system, both extracted from an energy-minimized α-helical fragment. The protons in the 6-spin system were the NH, αCH, and a βH of residue 1 and the NH and βH of residue two. The protons in the 15-spin model were the α, β, and NH protons of residues 1–3 along with the NH of residue 4 and the γH's of residue 2. Similar results were obtained with both models. The rotational correlation time derived from the ratio of the diagonal peak intensity for the NH of Glu14 to the cross-peak between the NH and the αH of Glu14 was 2.5 ns.

It would therefore appear that the rotational correlation time for motilin under the conditions used here (i.e., in 30% hexafluoropropanol) is between 1.2 and 2.5 ns, with the latter value reflecting the correlation time of the helical portion of the peptide and the shorter value for Pro3 indicating increased flexibility in the hydrophobic amino terminus. The 2.5-ns time is comparable to the correlation time of 2.2 ns predicted (Cantor & Schimmel, 1980) for an isotropically rotating peptide with a molecular weight of 2700 in 30% hexafluoro-2-propanol, which has a viscosity twice that of water (L. Qiu and J. Shriver, unpublished data). Thus it would appear that motilin under the conditions used here exists as a monomer.

One of the advantages of working with a protein the size of motilin is the effectiveness of the two-spin approximation for measuring distances. However, the small rotational correlation time results in relatively small NOESY cross-peaks. In order to make assignments with confidence, and particularly to investigate the existence of secondary structure in motilin, we have increased the signal/noise ratio of the NOESY cross-peaks by using relatively long mixing times, e.g., 450 ms. It is important to assess the effect of spin diffusion on the precision of the results obtained from the use of such long mixing times. Figure 9 shows the NOE cross-peak buildup curves expected for αH_i–NH_i, αH_i–NH_{i+1}, NH_i–NH_{i+1}, and αCH_i–NH_{i+3} NOE's in an α-helical (A) and extended-chain (B) segment in a peptide with a correlation time of 2.5 ns. Shown for comparison are the buildup curves for isolated two-spin systems with separations of 2.5, 2.8, 3.0, 3.5, 4.0, and 4.5 Å. Clearly, spin diffusion does have an effect, and the estimated error in distance determinations at mixing times of 450 ms can be on the order of 0.3–0.5 Å. However, these errors are not large enough to allow false assignments of secondary structure. (Not shown are the intensities of the diagonal peaks which decrease significantly over a period of 500 ms and become comparable in magnitude to the cross-peaks.) A more complete analysis of the buildup of NOESY cross-peaks in motilin will be presented elsewhere.

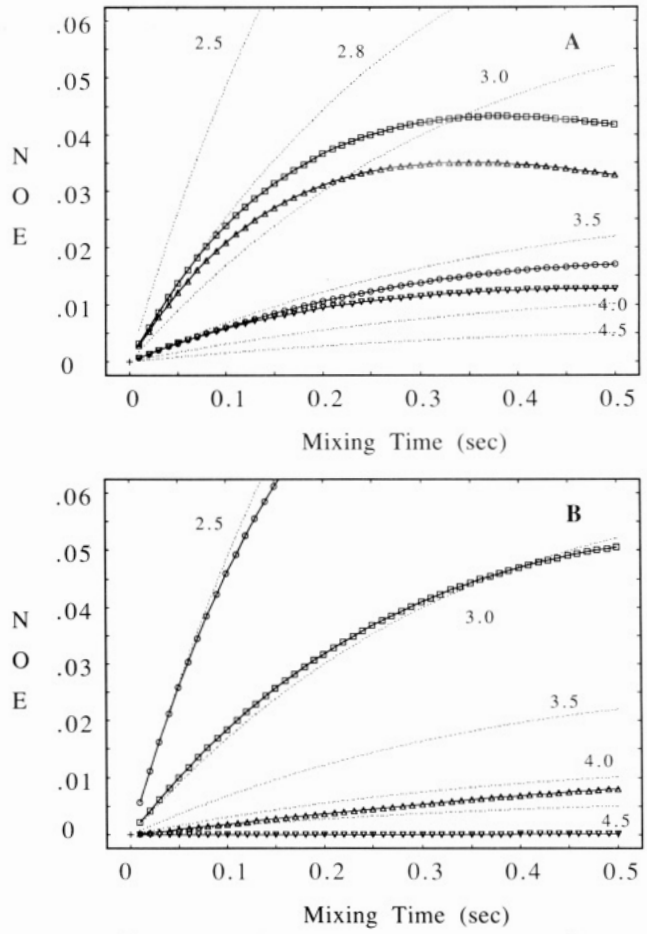

FIGURE 9: Simulations of the dependence of the intensities of the αCH_i–NH_i (□), αCH_i–NH_{i+1} (○), NH_i–NH_{i+1} (△), and αCH_i–NH_{i+3} (▽) NOESY cross-peaks on the mixing time (τ_m) for protons in an α-helix (A) and the extended chain (B) with a rotational correlation time of 2.5 ns (isotropic rotation is assumed). A grid of NOE curves (dotted lines) for isolated two-spin systems (τ_C = 2.5 ns) is shown for comparison with separations of 2.5, 2.8, 3.0, 3.5, 4.0, and 4.5 Å. The α-helix simulations in (A) used a 15-spin system (105 distances) extracted from an energy-minimized helix composed of glutamate, arginine, asparagine, and lysine (i.e., residues 17–20 of motilin, which comprise a region predicted to be in an α-helix according to the Chou–Fasman rules). The spins used in the simulation were the α and NH protons of the Glu, Arg, and Asn, the NH of Lys, the βH's of the Glu, Arg, and Asn, and the γH's of Arg. The four "backbone" proton cross-peaks had the following distances: αCH_i–NH_i, 2.76 Å; αCH_i–NH_{i+1}, 3.56 Å; NH_i–NH_{i+1}, 2.81 Å; αCH_i–NH_{i+3}, 3.53 Å. The extended-chain simulations in (B) used a 9-spin system (36 distances) extracted from an extended chain of the same four residues. The spins used were the NH and αCH of each residue along with two additional spins that could enhance the effects of spin diffusion: a γ proton on Glu (2.01 Å from the NH of Arg) and a γ proton on Arg (2.53 Å from the αCH of Arg). The four "backbone" proton cross-peaks had the following distances: αCH_i–NH_i, 2.94 Å; αCH_i–NH_{i+1}, 2.49 Å; NH_i–NH_{i+1}, 4.47 Å; NH_i–NH_{i+3}, 11.6 Å.

Discussion

The circular dichroism studies on motilin clearly indicate the presence of secondary structure in solution. Although a detailed analysis has not been performed on the CD data in this work, the shoulder at 222 nm indicates the presence of α-helical structure. The negative ellipticity band increases significantly with increasing concentrations of HFP, and the resulting CD spectrum is clearly indicative of α-helix. A more detailed analysis of the CD spectra will be presented elsewhere. The mean residue ellipticity of −18 000 deg·cm^2/dmol at 222 nm can be used to estimate an average α-helical content in motilin under conditions similar to those used in the NMR experiments. Using a mean residue ellipticity at 222 nm of +3900 deg·cm^2/dmol for random coil (Greenfield & Fasman, 1969) and −38 000 deg·cm^2/dmol for α-helix (Toniolo et al., 1979), we estimate the α-helical content of motilin to be about 50% in 30% HFP. A similar evaluation of the CD spectrum obtained in the absence of HFP gives an estimated α-helical content of 20%. The CD titration data (Figure 1) clearly show a narrow isodichroic region from 200 to 204 nm, which suggests that two major structural elements prevail: α-helix and random coil. However, since there is a isodichroic region rather than a point, the structural transition that occurs during the titration involves more than two elements. A more detailed analysis will be required to determine if the CD spectra support the presence of the reverse turn indicated by the NMR data.

The NMR studies presented here clearly indicate the location of the helical secondary structure indicated by the CD. Although the observation of a single NH_i–NH_{i+1} NOE connectivity does not indicate a unique structure, a sequential series of NH_i–NH_{i+1} NOE connectivities occur in regions of the peptide that exhibit α-helical structure (Wuthrich et al., 1984). More conclusive proof for α-helical structure is characterized by medium-range αCH_i–NH_{i+3}, NH_i–NH_{i+3}, and αCH_i–βCH_{i+3} NOE's (Billeter et al., 1982; Wuthrich et al., 1984; Wuthrich, 1986).

In motilin, sequential NH–NH NOE connectivities are observed from residues 6 to 10, 11 to 15, 17 to 19, and 20 to 22. Connectivities may be obscured between residues 5 and 6, 15 and 16, and 19 and 20 due to nearly coincident chemical shifts. No sequential NH–NH connectivities can be observed from residues 1 to 4 since the phenylalanine amino protons are in fast exchange with the solvent, and proline 3 has no amide proton. The observation of $i, i + 3$ αCH–NH NOESY cross-peaks from Glu9 to Lys20 (Figure 8) indicates the presence of α-helical structure which extends from residues 9 to 20. These results are in good agreement with the predicted α-helical structure obtained by using the Chou–Fasman method (Chou & Fasman, 1974a,b).

The unusual chemical shift of the amide resonance of isoleucine 4 suggests structure in the N-terminal hydrophobic region of motilin. In addition, the αCH resonance of phenylalanine 5 is shifted relatively far downfield near the water resonance. These observations, plus a weak NOE connectivity between the αCH of proline 3 and the NH of phenylalanine 5, a strong αCH–NH(3,4) connectivity, and a weak NH–NH(4,5) NOE, indicate a reverse turn conformation from residues 2 to 5 (Wuthrich et al., 1984; Dyson et al., 1988a). This would place proline 3 in position 2 of the turn, a very favorable position (Rose et al., 1985; Richardson, 1981). The low intensities of the αCH–NH(3,5) and NH–NH(4,5) NOE cross-peaks indicate that other conformations may be present as well. Restrained molecular dynamics studies are presently underway to clarify the structure of the peptide in this region as well as the rest of the molecule.

The distribution of charged residues in motilin is worth noting. Charged residues appear from residues 9 to 20, which corresponds to the helical region determined by the NMR study. Dipole, side-chain, and electrostatic interactions all contribute to helix stability (Shoemaker et al.,1987; Sundaralingam et al., 1985). Bierzynski et al. (1982) and Rico et al. (1984) in studies on ribonuclease S and C peptides have found salt bridges as helix-stabilizing factors. Salt bridges and ion pairs particularly have been found to stabilize helices in short, synthetic peptides (Marqusee & Baldwin, 1987). In a low dielectric constant environment charge pairs would be more strongly favored than in aqueous solution. In motilin, Glu9/Arg12, Glu15/Arg18, and Glu17/Lys20 are most likely to form salt bridges and ion pairs. We also note that the COOH-terminal region of the α-helix contains positively charged residues (arginine 18 and lysine 20) while the N-terminal has an acidic residue (glutamate 9). Such a placement of charge would stabilize the macrodipole of the helix, an important factor for helix stabilization on the basis of the helix dipole model (Shoemaker et al., 1987).

The estimated amount of α-helical structure from the CD data collected in 30% HFP (i.e., 50%) is essentially equal to that estimated from the NMR studies (i.e., 12 helical residues out of 22, or 54%). This indicates that in 30% HFP the peptide is predominantly in a single, stable α-helical structure, spanning residues 9–20. A more detailed analysis of NOE intensities and buildup rates is presently underway in order to more precisely define the structure of motilin in solution by using restrained molecular dynamics.

HFP has been used here to stabilize secondary structure which is thought to exist in aqueous solution. By stabilizing the structure with HFP, we are permitted a more complete characterization of the extent of the structure. Although it cannot be stated for certain at this point whether or not this structure is physiologically relevant, it is unlikely that a random coil conformation of the peptide hormone is active. Rather, it is more likely that the hormone adopts a conformation such as that defined here in its active form in aqueous solution in the vicinity of the membrane receptor.

ACKNOWLEDGMENTS

We thank Prof. V. Mutt, Department of Biochemistry II, Karolinska Institutet, Stockholm, Sweden, for his kind gift of porcine motilin and valuable discussions about the work. We also acknowledge Dr. Lennart Johansson and Niklas Lindskog for help with the CD measurements.

Registry No. Porcine motilin, 9072-41-7.

REFERENCES

Aue, W. P., Bartholdi, E., & Ernst, R. R. (1976) *J. Chem. Phys. 64*, 2229.

Bax, A., & Freeman, R. (1981) *J. Magn. Reson. 44*, 542.

Bax, A., & Drobny, G. (1985) *J. Magn. Reson. 61*, 306–320.

Bazzo, R., Tappin, M. J., Pastore, A., Harvey, T. S., Carver, J., & Campbell, I. D. (1988) *Eur. J. Biochem. 173*, 139–146.

Bierzynski, A., Kim, P. S., & Baldwin, R. L. (1982) *Proc. Natl. Acad. Sci. U.S.A. 79*, 2470.

Billeter, M., Braun, W., & Wuthrich, K. (1982) *J. Mol. Biol. 155*, 321–346.

Bloom, S. R., Christofides, N. D., Modlin, I., & Fitzpatrick, M. L. (1978) *Gastroenterology 74*, 1010.

Boelens, R., Koning, T., van der Marel, G., van Boom, J., & Kaptein, R. (1989) *J. Magn. Res. 82*, 290–308.

Braun, W., & Go, N. (1985) *J. Mol. Biol. 186*, 611–626.

Brown, J. C., Mutt, V., & Dryburgh, J. R. (1971) *Can. J. Physiol. Pharmacol. 49*, 399–405.

Brown, J. C., Cook, M. A., & Dryburgh, J. R. (1972) *Gastroenterology 62*, 401–404.

Brown, J. C., Cook, M. A., & Dryburgh, J. R. (1973) *Can. J. Biochem. 51*, 533.

Bundi, A., & Wuthrich, K. (1979) *Biopolymers 18*, 285–298.

Cantor, C., & Schimmel, P. (1980) *Biophysical Chemistry*, W. H. Freeman and Co., San Francisco.

Chou, P. Y., & Fasman, G. D. (1974a) *Biochemistry 13* (2), 211–222.

Chou, P. Y., & Fasman, G. D. (1974b) *Biochemistry 13*, (2), 222–245.

Christofides, N. D., & Bloom, S. R. (1981) in *Gut Hormones*, 2nd ed., Churchill Livingstone, Edinburgh.

Clore, G. M., & Gronenborn, A. (1989) *J. Magn. Reson. 84*, 398–409.

Clore, G. M., Martin, S. R., & Gronenborn, A. M. (1986) *J. Mol. Biol. 191*, 553.

Clore, G. M., Nilges, M., Brunger, A., Karplus, M., & Gronenborn, A. (1987) *FEBS Lett. 213*, 269–277.

Dea, D., Boileau, G., Poitras, P., & Lahaie, R. G. (1989) *Gastroenterology 96*, 695–703.

de Vlieg, J., Scheek, R., van Gunsteren, W., Berendsen, H., Kaptein, R., & Thomason, J. (1988) *Proteins 3*, 209–218.

Driscoll, P. C., Hill, H.A. O., & Redfield, C. (1987) *Eur. J. Biochem. 170*, 279–292.

Dyson, J., Rance, M., Houghten, R. A., Lerner, R. A., & Wright, P. E. (1988a) *J. Mol. Biol. 201*, 161–200.
Dyson, J., Rance, M., Houghton, R. A., Lerner, R. A., & Wright, P. E. (1988b) *J. Mol. Biol. 201*, 201–217.
Eich, G. W., Bodenhausen, G., & Ernst, R. R. (1982) *J. Am. Chem. Soc. 104*, 3731–3732.
Gooley, P. R., & MacKenzie, N. E. (1988) *Biochemistry 27*, 4032–4040.
Greenfield, N., & Fasman, G. D. (1969) *Biochemistry 8*, 4108–4116.
Havel, T. F., & Wuthrich, K. (1985) *J. Mol. Biol. 182*, 281–294.
Imura, H., Seino, Y., Mori, K., Itoh, Z., & Yanaihara, N. (1980) *Endocrinol. Jpn.*, S.R. No. 1, 151–155.
Jacobowitz, D. M., O'Donohue, T. L., Chey, W. Y., & Chang, T. M. (1981) *Peptides 2*, 363–369.
Jeener, J., Meier, H., Bachmann, P., & Ernst, R. R. (1979) *J. Chem. Phys. 71*, 4546–4553.
Keepers, J., & James, T. (1984) *J. Magn. Res. 57*, 404–426.
Kondo, Y., Torii, K., Omura, S., & Itoh, Z. (1988) *Biochem. Biophys. Res. Commun. 150*, (2), 877–882.
Kumar, A., Wagner, G., Ernst, R. R., & Wuthrich, K. (1980) *Biochem. Biophys. Res. Commun. 96*, 1156–1163.
Marqusee, S., & Baldwin, R. L. (1987) *Proc. Natl. Acad. Sci. U.S.A. 84*, 8898–8902.
Massefski, W., & Bolton, P. (1985) *J. Magn. Reson. 65*, 526–530.
Maxfield, F. R., & Scheraga, H. A. (1975) *Macromolecules 8*, 491.
McIntosh, C. H. S., & Brown, J. C. (1988) in *Advances in Metabolic Disorders* (Luft, R., Levine, R., & Mutt, V., Eds.) Vol. 11, pp 439–455, Academic Press, New York.
Mutt, V. (1982) *Vitam. Horm. (N.Y.) 39*, 231.
Nagayama, K., & Wuthrich, K. (1981a) *Eur. J. Biochem. 114*, 365–374.
Nelson, J. W., & Kallenbach, N. R. (1986) *Proteins: Structure, Function, and Genetics 1*, 211–217.
Ohe, K., Sumii, K., Sano, K., Kishimoto, S., & Miyoshi, A. (1980) *Endocrinol. Jpn.*, No. 1, 167–172.
Otting, G., Marchot, P., Bougis, P. E., Rochat, H., & Wuthrich, K. (1987) *Eur. J. Biochem. 168*, 603–607.
Poitras, P., Lahaie, R. G., St-Pierre, S., & Trudel, L. (1987) *Gastroenterology 92*, 658–662.
Rance, M., Bodenhausen, G., Wagner, G., Ernst, R. R., & Wuthrich, K. (1983) *Biochem. Biophys. Res. Commun. 117*, 479–485.
Richardson, J. S. (1981) *Adv. Protein Chem. 34*, 167–339.
Rico, M., Gallego, E., Santoro, J., Barmejo, F. J., Nieto, J. L. & Herranz, J. (1984) *Biochem. Biophys. Res. Commun. 123*, 757.
Rico, M., Santora, J., Bermejo, F. J., Herranz, J., Nieto, J. L., Gallego, E., & Jimenez, M. A. (1986) *Biopolymers 25*, 1031–1053.
Rose, G. D., Gierasch, L. M., & Smith, J. A. (1985) *Adv. Protein Chem. 37*, 1–105.
Sauriol, F., Lankin, D., & Patt, S. (1987) *Magn. Moments 3*, No. 2, 11–13.
Schubert, H., & Brown, J. C. (1974) *Can. J. Biochem. 52*, 7–8.
Shoemaker, K. K., Kim, P. S., York, E. J., & Baldwin, R. L. (1987) *Nature (London) 326*, 563–567.
States, D. J., Haberkorn, R. A., & Ruben, D. J. (1982) *J. Magn. Reson. 48*, 286–292.
Sunderalingam, M., Drendel, W., & Greaser, M. (1985) *Proc. Natl. Acad. Sci. U.S.A. 82*, 7944–7947.
Tappin, M. J., Pastore, A., Norton, R. S., Freer, J. H., & Campbell, I. D. (1988) *Biochemistry 27*, 1643–1647.
Toniolo, C., Bonora, G. M., Salardi, S., & Mutter, M. (1979) *Macromolecules 12*, 620–625.
Ueda, K., Kitagawa, K., Akita, T., Honma, S., Segawa, T., Kai, Y., Mori, Y., & Yajima, H. (1977) *Chem. Pharm. Bull. 25*, 2123–2126.
Usellini, L., Buchan, A. M. J., Polak, J. N., Capella, C., Cornaggiaa, M., & Solcia, E. (1984) *Histochemistry 81*, 363–368.
Wagner, G. (1983) *Q. Rev. Biophys. 16*, 1–57.
Wagner, G., & Wuthrich, K. (1982) *J. Mol. Biol. 155*, 347–366.
Wagner, G., Neuhaus, D., Worgotter, E., Vasak, M., Kagi, J. H. R., & Wuthrich, K. (1986) *J. Mol. Biol. 187*, 131–135.
Wider, G., Hosur, R. V., & Wuthrich, K. (1983) *J. Magn. Reson. 52*, 130–135.
Wright, P., Dyson, H., & Lerner, R. (1988) *Biochemistry 27*, 7167–7175.
Wuthrich, K. (1986) *NMR of Proteins and Nucleic Acids*, J. Wiley and Sons, New York.
Wuthrich, K., Billeter, M., & Braun, W. (1984) *J. Mol. Biol. 180*, 715–740.
Zuiderweg, E. R. P., Hallenga, K., & Olejniczak, E. T. (1986) *J. Magn. Reson. 70*, 336–343.